NISTIR 5838

Room-Temperature Thermal Conductivity of Expanded Polystyrene Board for a Standard Reference Material

R.R. Zarr, M.W. Davis, and E.H. Anderson
Building and Fire Research Laboratory
Gaithersburg, Maryland 20899

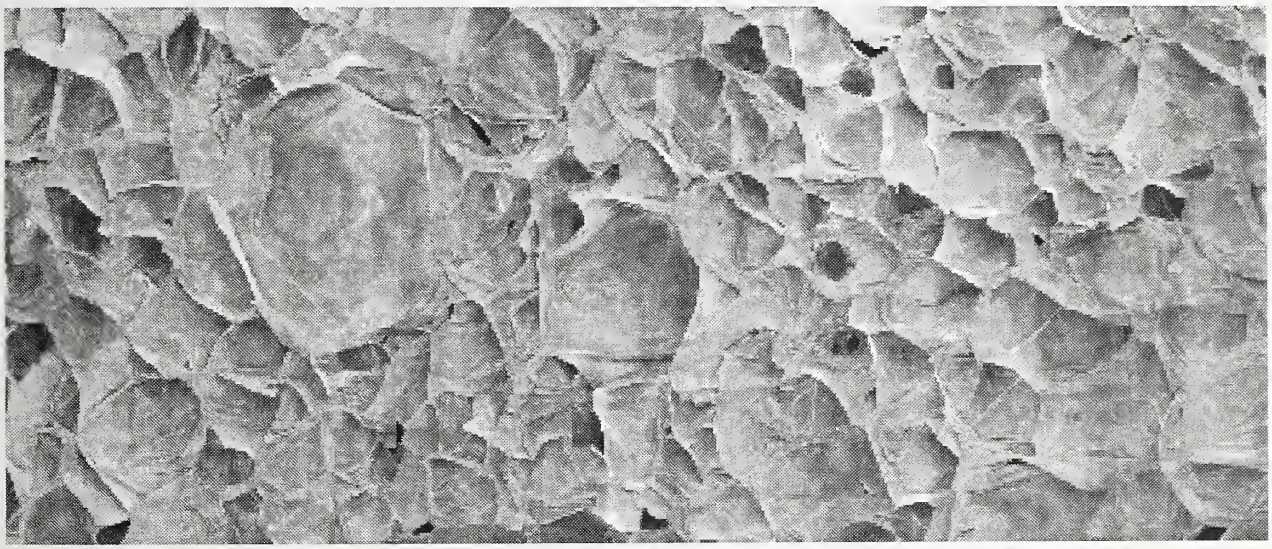

NIST

United States Department of Commerce
Technology Administration
National Institute of Standards and Technology

NISTIR 5838

Room-Temperature Thermal Conductivity of Expanded Polystyrene Board for a Standard Reference Material

R.R. Zarr. M.W. Davis. and E.H. Anderson

May 1996
Building and Fire Research Laboratory
National Institute of Standards and Technology
Gaithersburg, Maryland 20899

U.S. Department of Commerce
Ronald H. Brown, *Secretary*
Technology Administration
Mary L. Good, *Under Secretary for Technology*
National Institute of Standards and Technology
Arati Prabhakar, *Director*

Abstract

Thermal conductivity measurements at room temperature are presented as the basis for certified values of SRM 1453, expanded polystyrene board. The measurements have been conducted in accordance with a randomized full factorial experimental design with two variables, bulk density and temperature, using NIST's one-meter line-heat-source guarded hot plate apparatus. Uncertainties of the measurements, consistent with current ISO guidelines, have been prepared. The thermal conductivity measurements were conducted over a range of bulk density of 37.4 to 45.8 kg/m^3 and mean temperature of 281 to 313 K. Statistical analyses of the physical properties of the SRM are presented and include variations between boards, as well as within boards. Measurements of the foam's compressive properties and microstructure are presented.

Table of Contents

1. Introduction

A Standard Reference Material (SRM) is a homogeneous and stable material which is measured accurately and certified as a reference material for purposes of evaluating a measurement process [1]. Thermal insulation SRMs provide certified values of thermal conductivity and resistance over a range of parameters, such as density and temperature. SRMs are intended primarily as a method for providing measurement assurance to user communities; for example, assistance in the calibration of heat-flow-meter apparatus and operation of guarded hot plate apparatus (ASTM Test Methods C 518 and C 177, respectively). The systematic use of common SRMs, including proper tracking with control charts, provides the means for accurate interlaboratory comparison of thermal conductivity data.

New SRMs are developed, usually after a formal request, in order to satisfy the measurement needs of a user community. Obviously, the need must be clearly demonstrated in order to justify issuing an SRM. The motivation for SRM 1453, expanded polystyrene board, began during the development of the ASTM Test Method C 1199 [2] for the thermal evaluation of fenestration systems (windows and doors). The method requires the use of a large calibration transfer standard having known thermal transmission properties in order to estimate the surface heat transfer coefficients of more complex fenestration systems. The motivation intensified when the Energy Policy Act of 1992 [3] mandated that a voluntary window rating program be developed by the National Fenestration Rating Council (NFRC) according to accepted national testing procedures.

On March 11, 1993, representatives from NFRC, industry, and the National Voluntary Laboratory Accreditation Program (NVLAP) met at the National Institute of Standards and Technology (NIST) to discuss a proposal for a new SRM. The primary purpose of the new SRM would be to assist the thermal testing community in the thermal evaluation of fenestration systems, especially windows. As part of the meeting, the representatives discussed an experimental design for development of the SRM (described later) and the mechanical design for a recommended calibration transfer standard. The design for the transfer standard was based on work done at the National Research Council of Canada [4] and consisted of 13-mm thick expanded polystyrene foam (density of 20 kg/m^3) laminated to 3-mm glass sheets on either side [5].

Preliminary measurements were conducted by NIST on six specimens of a candidate material of molded expanded polystyrene foam provided by industry. The bulk density of the specimens ranged from 41 to 49 kg/m^3 and the average thermal conductivity (at 24 °C) for the six specimens was 0.033 W/m·K. The effect of density on thermal conductivity was found to be fairly insensitive. Based on these preliminary studies, NIST procured a large number of boards of molded expanded polystyrene foam for development as SRM 1453. This report describes the specimens, experimental design, measurement procedures, and test results. Uncertainty analyses of the measurements are included in the Appendices.

2. Specimens

Test specimens for characterizing the thermal transmission properties of SRM 1453 were selected from a single lot of a commercial grade of molded expanded polystyrene foam boards. The selection of test specimens was based on an experimental design provided by the Statistical Engineering Division at NIST. This section describes the production of the boards, their physical properties, including inhomogeneities between and within boards, the foam's cellular microstructure and surface texture, and selection of test specimens.

Manufacture and Surface Preparation

In April of 1994, NIST purchased 300 boards of molded polystyrene foam from Polyfoam, Incorporated[1]. The material was manufactured by expanding (by heating) particles of a polystyrene polymer saturated with a volatile hydrocarbon, such as isopentane. The expanded beads were subsequently placed in a plank mold and heated under pressure until the beads fused together. To remove surface imprints from the molding process, the boards were shipped directly to a finishing company where both sides of each board were sanded using a modified milling machine in order to obtain a uniform thickness. The final nominal dimensions of the boards were 930 by 660 mm by 13 mm thick. On November 10, 1994, the boards were delivered to NIST and placed in a storage room maintained at 21 °C ± 2 °C and a relative humidity that ranged from 30 to 60 percent.

Statistical Characterization of Physical Properties

In order to select the test specimens for this study, it was necessary to determine the mass, physical dimensions, and bulk density of each board of polystyrene foam. Table 1 gives summary statistics

Table 1
Summary Statistics for Expanded Polystyrene Boards (n = 300)

	Mass	Length	Width	Thickness	Bulk Density
	(g)	(mm)	(mm)	(mm)	(kg/m^3)
Average	328.3	930.65	656.90	13.23	40.60
Std. Dev.	16.9	0.04	0.13	0.13	2.05
Maximum	371.1	931.5	658.0	14.12	45.7
Minimum	285.1	927.5	636.5	12.71	35.2

[1] Certain commercial equipment, instruments, or materials are identified in this report to specify adequately the experimental procedure. Such identification does not imply recommendation or endorsement by NIST, nor does it imply that the materials or equipment are necessarily the best for the purpose.

for the mass, length, width, thickness, and bulk density of the 300 boards. One board, identified as 049, had an unusually low density (Table 1). This board was subsequently identified as an outlier, removed from the lot, and used for supplemental measurements that included scanning electron microscopy and surface texture measurements described below.

Variations Between Boards

Variations in the thickness and bulk density from board-to-board were analyzed graphically using a four-step method. The method consisted of 1) a run-sequence plot that checked for systematic and random changes; 2) a lag plot that checked for randomness; 3) a histogram that checked the frequency distribution; and, 4) a normal probability plot that checked for the normality assumption. Examples of the method are illustrated in Figures 1 and 2 for the board thickness and bulk density, respectively.

The data in Figure 1 reveal that, with the exception of five boards greater than 13.5 mm, the thickness of the 300 boards is, in general, very consistent from board-to board. The distribution of thicknesses is random as shown by the tight cluster ("bull's-eye") of data points in the center of the lag plot. Further, the distribution is normally distributed as shown in the histogram and normality plot about a mean value of 13.23 mm (see Table 1 for summary statistics).

The run sequence plot in Figure 2 shows that the bulk density also appears consistent from board-to-board. However, the lag plot reveals localized clusters of data points indicating that the distribution of data is skewed, particularly toward the lower bulk densities. The histogram confirms this observation and shows two peaks, a large peak at about 39 kg/m^3 and a smaller peak near 43 kg/m^3. Despite this distribution skew, for all practical purposes, the summary statistics provided in Table 1 suffice in describing the bulk density of the lot. The normality plot was used to identify board 049 as an outlier (Figure 2).

Variations Within a Board

The density variation with respect to position within a board was examined by dividing board 049 into 35 equal-size specimens, each 127 mm square. The bulk density of each 127 mm square specimen was determined and the variation examined using the plots shown in Figure 3. The histogram again reveals two peaks, a large peak near 36 kg/m^3 and a smaller one near 33 kg/m^3. In this case, the large and small peaks probably corresponded to density variations within board 049. The mean bulk density for the board was 35.09 kg/m^3 (slightly lower than the minimum value in Table 1) and the standard deviation was 2.26 kg/m^3. The variation of bulk density within board 049 is illustrated with the contour plot shown in Figure 4. The higher values of bulk density were near the center of the board and the lower values of bulk density were near the edges and corners of the board.

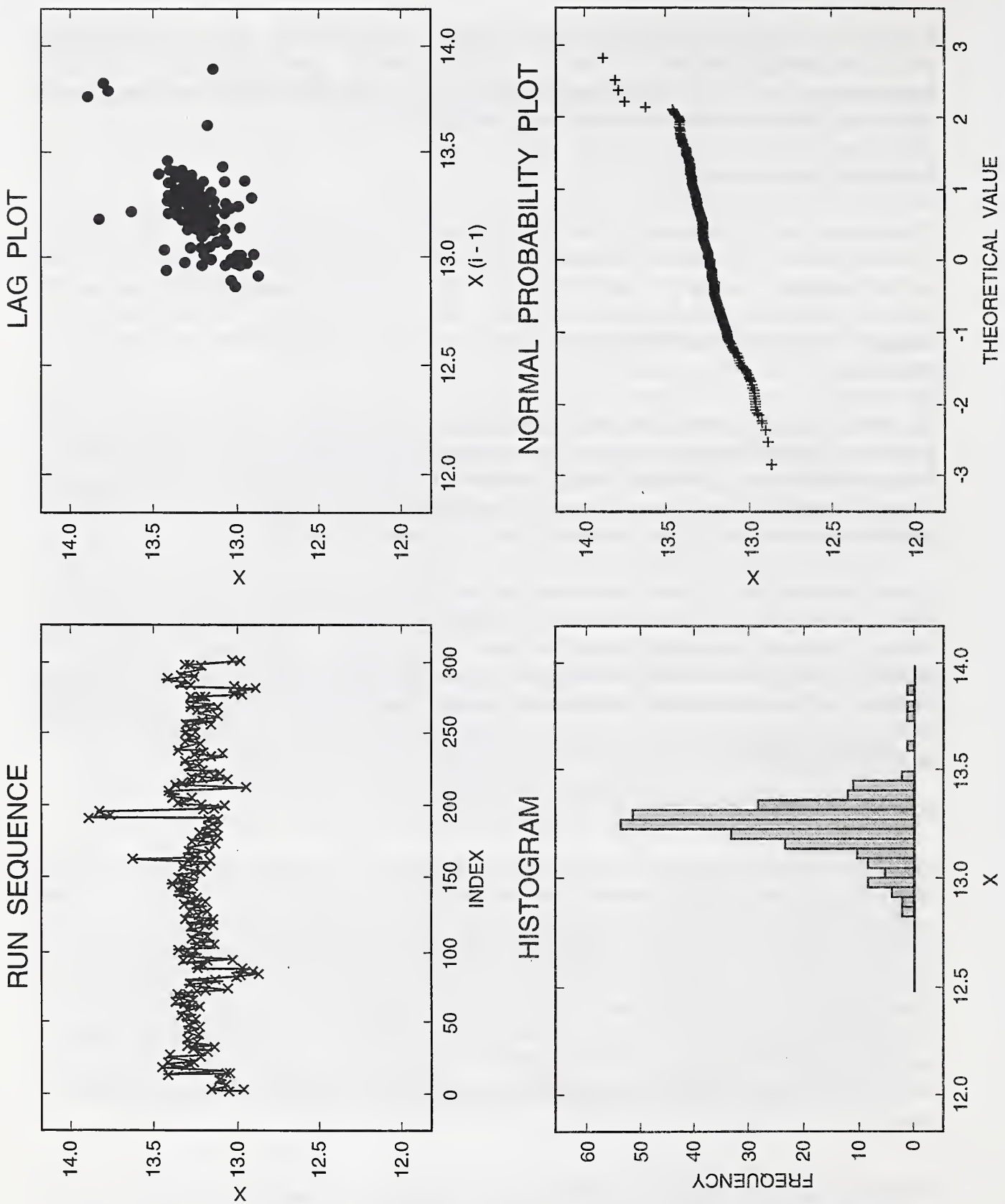

Figure 1. Global (between boards) variations of thickness; $\overline{L}$ = 13.23 mm, s($\overline{L}$) = 0.13 mm; n = 300.

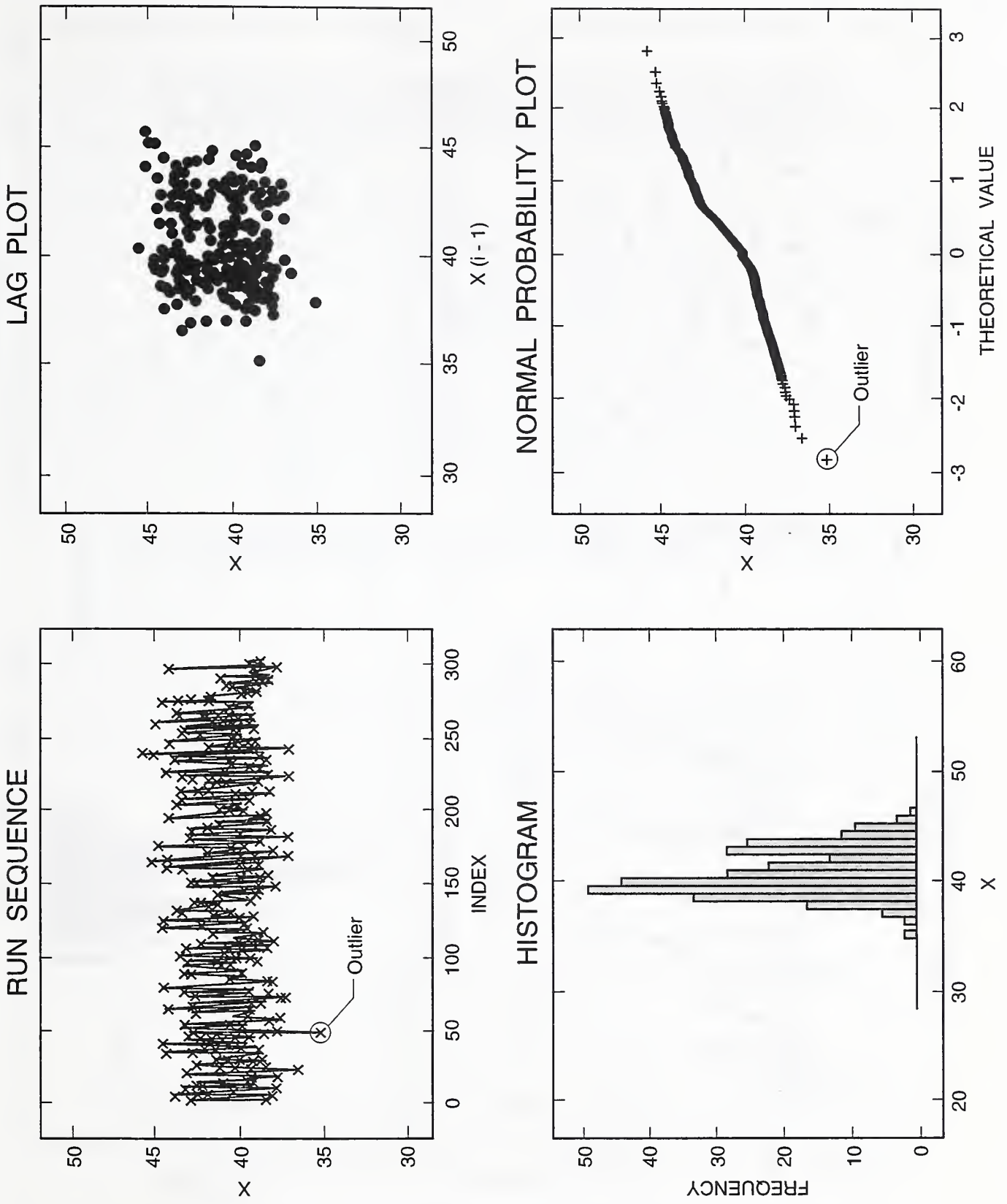

Figure 2 . Global (between boards) variations of bulk density; $\overline{\rho}$ = 40.60 kg/m^3; s ($\overline{\rho}$) = 2.05 kg/m^3; n = 300.

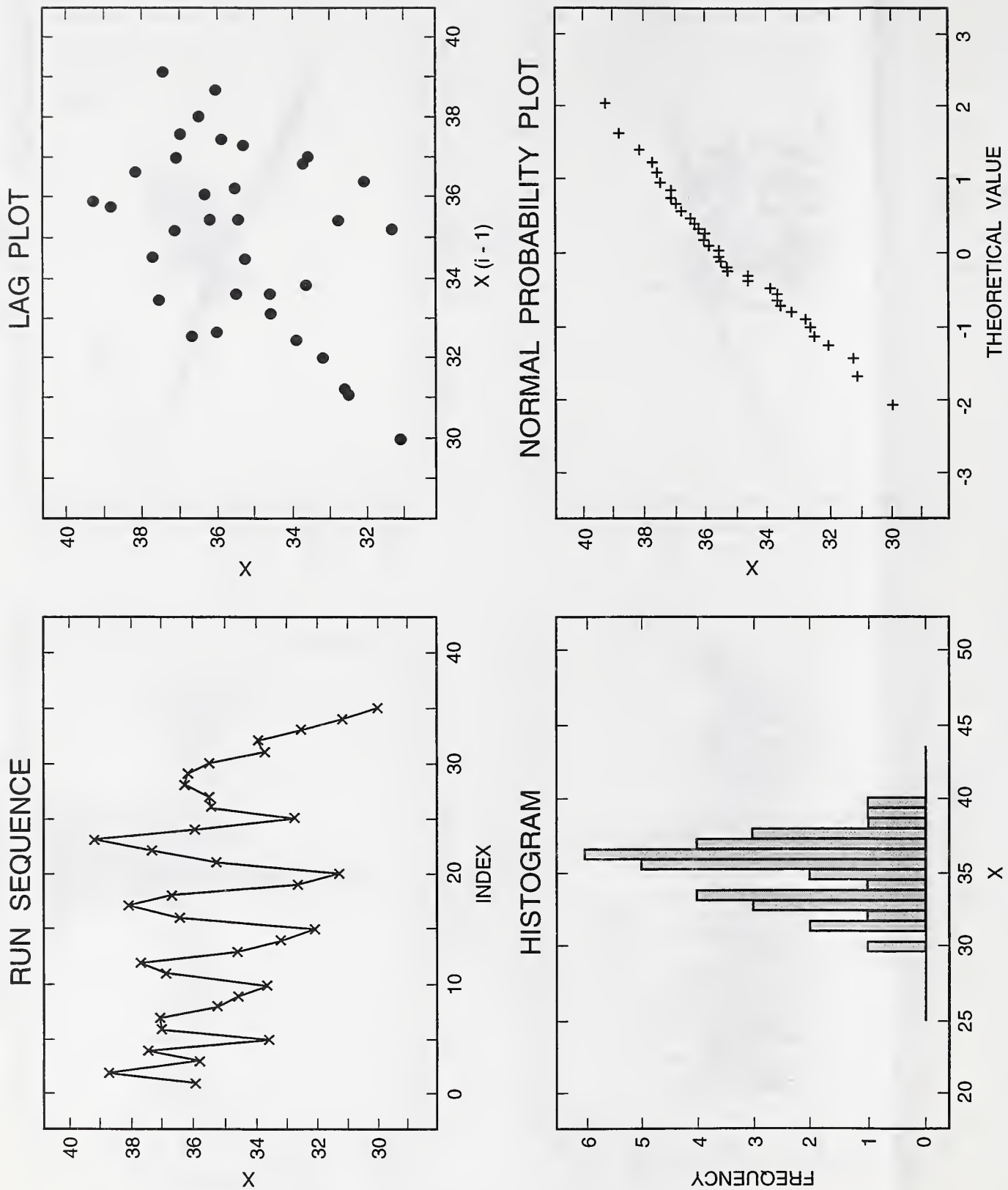

Figure 3 . Local (within board) variations of bulk density for board 049; $\overline{\rho}$ = 35.09 kg/m^3; s ($\overline{\rho}$) = 2.26 kg/m^3; n = 35.

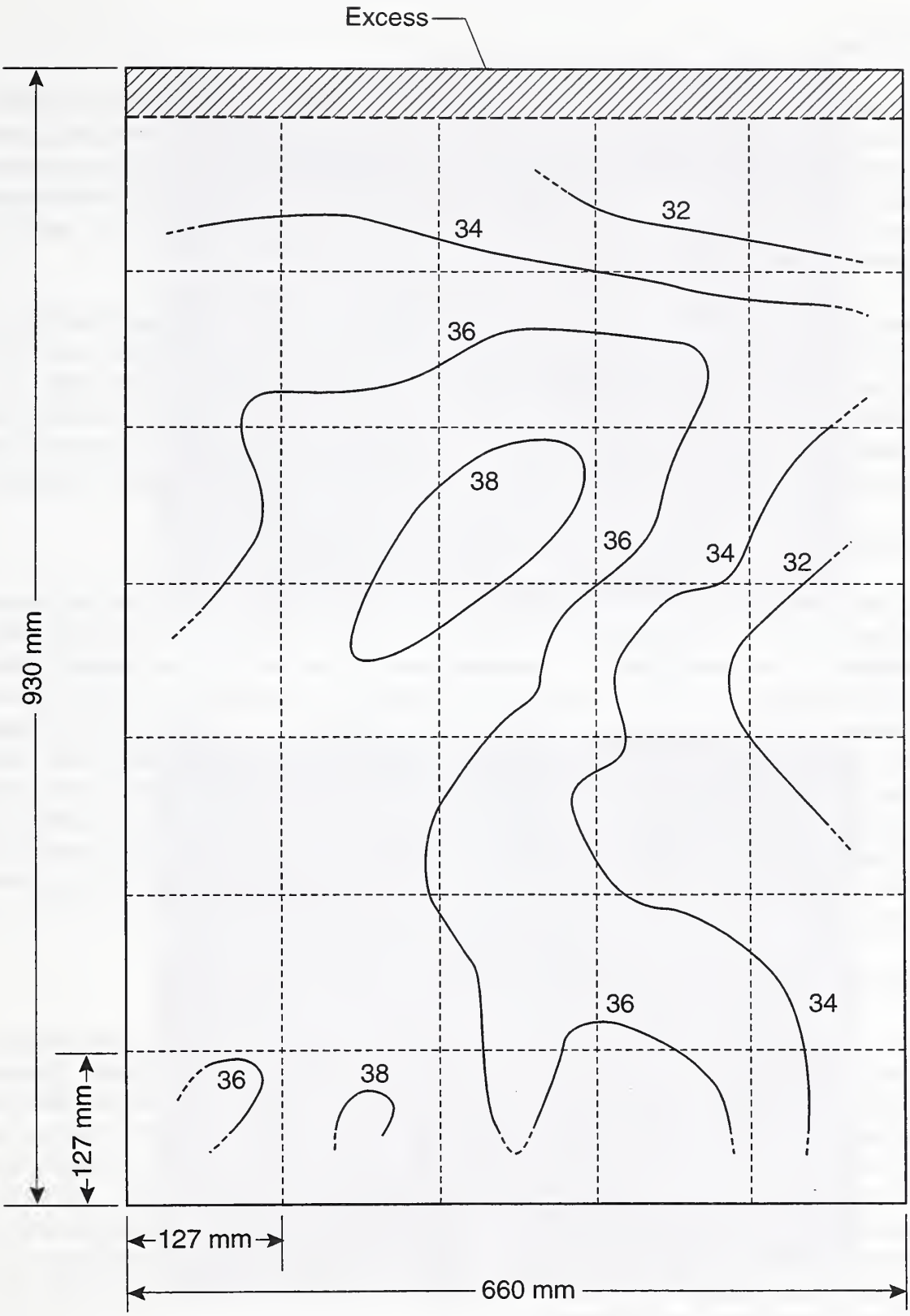

Figure 4. Contour plot for density variations (in kg/m^3) within board 049.

Microstructure

The microcellular structure of the foam was examined using a scanning electron microscope (SEM). Small specimens of foam, approximately 5 by 13 by 28 mm, were cut from one board using a razor blade and were subsequently sputter-coated with a 20 nm film of gold to prevent surface charging. Secondary electron images of the surface topography were obtained under operating conditions of 4 keV and a current of about 500 pA. Two images of the foam, at magnifications of 25x and 100x, respectively, are shown in Figure 5.

In Figure 5a, interfacial outlines indicate where the beads of expanded polystyrene fused together during the molding process. The size of the beads ranged from 1 to 3 mm and the voids at the intersection of three or more beads were relatively small as noted in the micrograph. At a magnification of 100x, Figure 5a reveals the distribution of microcells formed within the beads during the expansion process. The cells ranged typically from 0.02 to 0.4 mm. As evident in the micrograph, a large percentage of the cell walls were intact indicating a high closed-cell content.

Surface Roughness

The surface texture of the foam was examined by the staff of the NIST Precision Engineering Division with a Form Talysurf[1] instrument that generated a surface profile of the foam by means of a contact stylus. A specimen of foam, 127 mm square, was cut from board 049 and securely fastened relative to the instrument's stylus. The stylus was traversed over a sampling interval of the foam at three locations. Displacements of the stylus in the z-direction (i.e., parallel to the specimen thickness) were referenced to a filtered mean line, thus generating a series of peaks and valleys comprising the surface texture of the foam. The filter was a standard 2RC type with a nominal cutoff of 2.5 mm [6]. The average roughness, R_a [6], of the foam's surface was defined as the mean of the absolute values of the profile height deviations. The values of R_a at the three locations were 16, 20, and 16 μm. By comparison, values of R_a at three locations for a similar polystyrene foam *without* its surfaces sanded were 72, 80, and 82 μm, respectively.

Selection of Sample Lot for Thermal Conductivity Measurements

The goal in selecting the test specimens was to reduce the possibility of the user having to extrapolate outside the range of values of bulk density given in the SRM 1453 certificate. Therefore, it was necessary to weigh each board and determine its physical dimensions so that the entire lot of 300 boards could be rank ordered by bulk density. Three nominal levels of density were selected. The breakdown for the specimens consisted of five pairs having the lowest density (excluding board 049), five pairs about the median density, and five pairs having the highest density. Each pair of specimens had nearly the same bulk density. The 30 boards were subsequently cut using a table saw to dimensions of 657 mm square. Small changes in the density between the board size and the specimen size were noted and are summarized in Table 2. The maximum difference in bulk density for each pair of specimens was 2.2 percent.

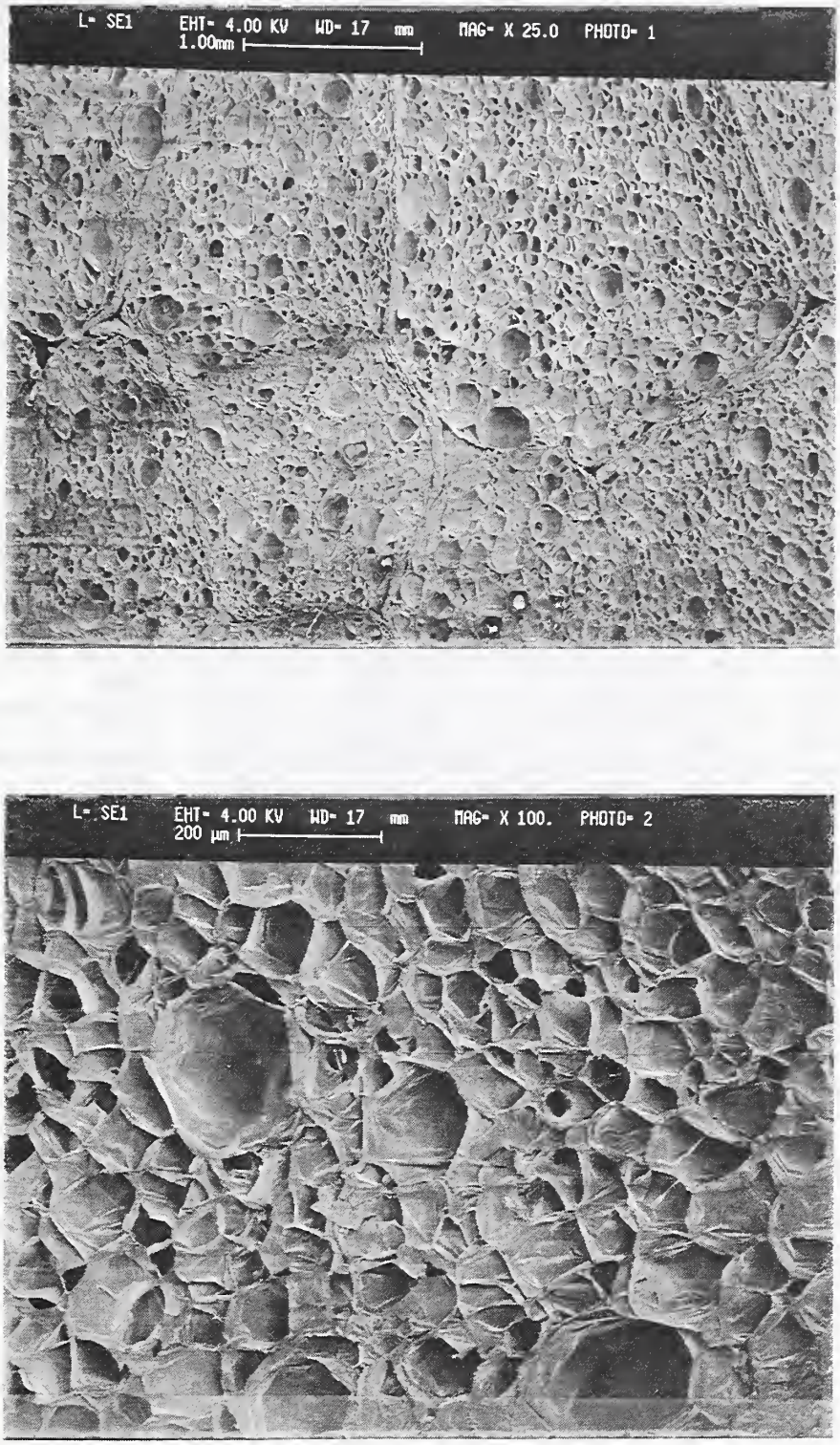

Figure 5. Microstructure of expanded polystyrene foam. (a) Magnification 25 x
(b) Magnification 100x

Table 2 Density Measurements of Specimens of Expanded Polystyrene Board									
Pair	Nominal Density Level	ID 1	ID 2	Board Density 1	Board Density 1	Diff.	Specimen Density 1	Specimen Density 2	Diff.
				(kg/m^3)	(kg/m^3)	(%)	(kg/m^3)	(kg/m^3)	(%)
1	Low	23	182	36.6	37.6	0.9	35.9	36.7	2.2
2	Low	168	242	37.0	37.1	0.2	36.8	36.6	0.4
3	Low	73	223	37.3	37.1	0.7	37.7	36.6	2.1
4	Low	59	72	37.5	37.6	0.1	37.6	37.7	0.4
5	Low	19	297	37.7	37.6	0.1	37.9	37.9	0.2
6	Mid	104	156	40.0	39.9	0.0	40.1	36.7	1.0
7	Mid	38	258	40.0	40.0	0.0	40.0	36.6	1.0
8	Mid	126	251	40.0	40.1	0.1	40.1	39.4	1.8
9	Mid	113	210	40.1	40.1	0.9	35.9	39.4	0.0
10	Mid	202	297	40.1	40.1	0.1	39.7	39.9	0.6
11	High	80	120	44.4	44.6	0.1	44.1	43.5	1.4
12	High	42	164	44.6	44.6	0.1	44.3	44.4	0.3
13	High	176	260	44.7	44.8	0.1	44.2	43.8	1.1
14	High	165	238	45.1	45.0	0.4	44.4	44.3	0.2
15	High	239	240	45.2	45.7	1.1	44.4	45.0	1.2

3. Experimental

Thermal conductivity measurements of the expanded polystyrene specimens were determined in accordance with ASTM Test Method C 177 using NIST's one-meter guarded hot plate apparatus. Each pair of test specimens was measured once in a fully randomized sequence in order to minimize the introduction of bias in the test results. The measurements were generally completed in one to two days. This section describes the measurement procedure, uncertainties, and experimental design.

Measurements of Thermal Conductivity

A schematic of the NIST one-meter line-heat-source guarded hot plate apparatus is shown in Figure 6. The apparatus has been described previously [7,8] and its operation is summarized briefly, here. Two specimens having nearly the same density, size, and thickness are placed on either side of the guarded hot plate and clamped securely by the circular cold plates. Ideally, the guarded hot

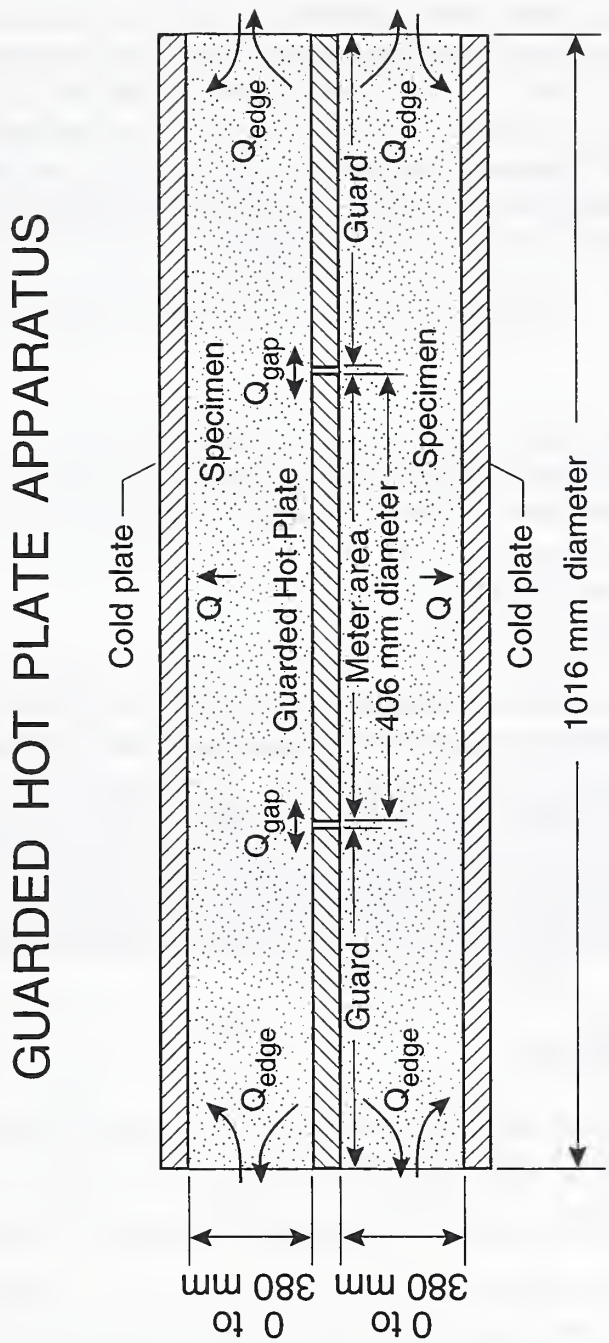

Figure 6 . Schematic of NIST one-meter guarded hot plate.

plate and cold plates provide constant-temperature boundary conditions to the surfaces of the specimens. With proper guarding in the lateral direction, the apparatus is designed to provide one-dimensional heat flow (Q) through the meter area of a pair of specimens.

During testing, data for Q and the plate temperatures were collected every two minutes. When the plate temperatures were within 0.05 K of their target temperatures and Q no longer changed monotonically, (steady-state) data were collected for four hours and averaged over the time interval. Measurements of (apparent)[2] thermal conductivity (λ) for the pair of specimens were determined in accordance with ASTM Test Method C 177 [8] using the following equation.

$$Q = \lambda A \frac{\Delta T}{L} \qquad (1)$$

where;

Q = heat flow through the meter area of the specimens, W;
A = meter area normal to direction of heat flow, m^2;
$\Delta T = T_h - T_c$, temperature difference across specimens, K;
T_h = hot plate temperature, K;
T_c = cold plate temperature, K; and,
L = thickness of specimens, m.

Values of λ were reported at the mean temperature (T) of the hot and cold plates, $T = \frac{1}{2}(T_h + T_c)$. The foam specimens, which were nominally 657 mm square, were installed in the apparatus and encircled with fibrous polyester blanket insulation. This material was selected because of its compressibility and similar thermal conductivity. In a separate series of guarded hot plate tests, the thermal conductivity of a pair of 13.3 mm-thick specimens of fibrous polyester was determined to be 0.0342, 0.0371, and 0.0403 W/m·K at mean temperatures of 281, 297 and 313 K, respectively. The effect of the fibrous polyester insulation on λ was included in the uncertainty analysis described in Appendix A.

Measurements of Bulk Density

The bulk density (ρ) of the foam specimens was determined using ASTM Test Method D 1622 [10] by dividing the mass (m) of the specimen by its volume (V), or;

$$\rho = \frac{m}{V} \qquad (2)$$

---

[2] The thermal transmission properties of heat insulators determined from standard test methods typically include several mechanisms of heat transfer, including conduction, radiation, and possibly convection. For that reason, some experimentalists will include the adjective "apparent" when describing thermal conductivity. However, for brevity, the term thermal conductivity shall be used in this report.

The specimen mass was obtained from a precision balance having a sensitivity of 0.1 g. The length and width of the specimen were measured at three locations using a steel rule having a resolution of 0.5 mm. The thickness was averaged from five measurements taken on a granite flat table with a precision caliper, 0.1 mm resolution. Corrections for the effect of the buoyant force on the polystyrene solid polymer were estimated to be 0.1 percent and neglected.

Uncertainty in Measurements

The measurement uncertainties for thermal conductivity, mean temperature, and bulk density were derived in accordance with current ISO guidelines [11,12] and described in Appendices A and B, respectively. The standard uncertainties for the thermal conductivity, mean temperature, and bulk density were 0.00012 W/m·K, 0.024 K, and 0.10 kg/m^3, respectively.

Design

Based on previous experience, a model for thermal conductivity (λ), bulk density (ρ), and mean temperature (T) was assumed to be

$$\lambda(\rho,T) = a_0 + a_1\rho + a_2T + a_3T^2 + a_4T^3 \qquad (3)$$

In order to check the adequacy of Equation (3), a full factorial design with 3 levels for ρ and 5 levels for T was selected, Table 3. This design also allowed us to check the necessity of: a quadratic term for ρ, a fourth-order term for T, and/or a cross-product term for ρ and T in order to model the data.

Table 3
Full Factorial (3 by 5) Experimental Design
Number of replicates, Test sequence

Density Level	Temperature Level (K)				
	281	289	297	305	313
High	1, (03)	1, (04)	1, (15)	1, (12)	1,(13)
Mid	1, (05)	1, (11)	1, (01)	1, (10)	1, (08)
Low	1, (14)	1, (07)	1, (09)	1, (06)	1, (02)

As noted in Table 3, three nominal levels of ρ were chosen that included the upper and lower extremes of the production lot. The lower value for temperature was essentially fixed by the low limit of the guarded hot plate apparatus at 281 K. Unfortunately, the value of 281 K is somewhat higher than the low temperature values specified in ASTM Test Method C 1199 [2]. An upper temperature limit of 313 K was chosen based on the technical information provided in the ASTM material specification for cellular polystyrene thermal insulation [13].

4. Results

The fifteen pairs of expanded polystyrene specimens were tested in the guarded hot plate apparatus according to the test sequence given in Table 4. The identifiers, 1 and 2, refer to the top and bottom specimen, respectively. The average bulk density was computed for each pair of specimens and ranged from 36.3 to 44.7 kg/m^3.

Table 4
Test Sequence (Fully Randomized) for Specimen Pairs of Expanded Polystyrene

Test Sequence	Test Number	T	Nominal Density Level	ID 1	Specimen Density 1	ID 2	Specimen Density 2	Average Density
		(K)			(kg/m^3)		(kg/m^3)	(kg/m^3)
1	95-018A	297	Mid	**104**	40.1	**156**	39.7	39.9
2	95-019A	313	Low	**073**	37.7	**223**	36.6	37.3
3	95-020A	281	High	**080**	44.1	**120**	43.5	43.8
4	95-021A	289	High	**239**	44.4	**240**	45.0	44.7
5	95-022A	281	Mid	**038**	40.0	**258**	39.6	39.8
6	95-023A	305	Low	**059**	37.9	**072**	37.7	37.7
7	95-024A	289	Low	**168**	36.8	**242**	36.6	36.7
8	95-025A	313	Mid	**126**	40.1	**251**	39.4	39.8
9	95-026A	297	Low	**023**	35.9	**182**	36.7	36.3
10	95-027A	305	Mid	**113**	39.9	**210**	39.9	39.9
11	95-028A	289	Mid	**202**	39.7	**207**	39.9	39.8
12	95-029A	305	High	**176**	44.2	**260**	43.5	44.0
13	95-030A	313	High	**042**	44.4	**164**	44.4	44.3
14	95-031A	281	Low	**019**	37.9	**207**	37.9	37.9
15	95-032A	297	High	**165**	44.4	**238**	44.3	44.3

Table 5 summarizes the experimental test conditions and measured thermal conductivity (λ) for each pair of specimens. Note that an extra digit is provided for λ to reduce rounding errors. Each test was conducted with heat flow in the vertical direction and a temperature difference of 20 K across the specimens. During a test, the ambient temperature (T_a) of the air surrounding the specimens was maintained at the same value of the mean temperature (T) by means of a temperature-controlled environmental chamber. The ambient air pressure (P_a) was not controlled and varied with barometric conditions. The relative humidity (RH) varied with the chamber's dry-bulb temperature.

Several parameters in Table 5 indicate the "average" value for the top and bottom specimen, i.e., bulk density (ρ), thickness (L), clamping load, etc. The average thickness (L) was determined from in-situ measurements of the top and bottom plate separation. The grand average of the test

thicknesses was 13.43 ± 0.11 mm (one standard deviation). The grand average of the clamping loads was 477 N. This parameter varied from test-to-test (Table 5) due to the thermal expansion and contraction of the specimens and the apparatus. The maximum clamping pressure (load divided by the plate area) was well below the mechanical yield point of the polystyrene foam (Appendix C).

Table 5
Thermal Conductivity Measurements of SRM 1453, Expanded Polystyrene Board

Test	T	Average ρ	Average L	Average Load*	T_a	P_a	RH	T_h	Average T_c	Measured λ
	(K)	(kg/m^3)	(mm)	(N)	(K)	(kPa)	(%)	(K)	(K)	(W/m·K)
1	297	39.9	13.32	407	297.2	100.49	14	307.15	287.15	0.03349
2	313	37.3	13.29	714	313.2	101.15	8	323.15	303.15	0.03541
3	281	43.8	13.29	454	281.2	101.27	24	291.15	271.15	0.03159
4	289	44.7	13.52	140	289.2	101.33	10	299.15	279.15	0.03236
5	281	39.8	13.30	362	281.2	101.37	23	291.15	271.16	0.03170
6	305	37.7	13.30	594	305.2	100.28	10	315.15	295.15	0.03454
7	289	36.7	13.46	297	289.2	101.38	17	299.15	279.15	0.03271
8	313	39.8	13.44	736	313.2	101.11	8	323.15	303.15	0.03552
9	297	36.3	13.53	422	297.2	100.52	13	307.15	287.15	0.03373
10	305	39.9	13.52	685	305.2	100.25	10	315.15	295.15	0.03455
11	289	39.9	13.61	236	289.2	100.46	10	299.15	279.15	0.03263
12	305	44.0	13.48	632	305.2	100.43	10	315.15	295.15	0.03430
13	313	44.3	13.41	715	313.2	100.08	8	323.15	303.15	0.03511
14	281	37.9	13.30	324	281.2	100.79	24	291.15	271.16	0.03163
15	297	44.3	13.53	431	297.2	100.43	12	307.15	287.16	0.03330

* Plate Surface Area = 0.811 m^2.

5. Analysis

ASTM Test Method C 177 [8] recommends that, whenever possible, the bulk density of the specimen be determined for the volume corresponding to the meter area of the apparatus. Thus, a nominal 406-mm diameter cylinder was cut from a limited number of specimens to account for differences in the bulk densities of the meter area and the specimen. This section describes the correction for the specimen bulk density, plots of the specimen thermal conductivity, and regression analysis of the data.

Meter Area Bulk Density Correction

In order to reserve a few specimens for future measurements, only eight specimens (4 pairs) were selected for cutting. Using a jigsaw, 406-mm diameter cylinders were cut from the center of each specimen and the bulk density determined using Equation (2). Table 6 summarizes the bulk

densities of the specimen and meter area (406-mm diameter cylinder). The differences ranged from 0.1 to 1.9 kg/m^3 (0.2 to 5.2 percent).

Table 6
Comparison of Specimen and Meter Area Bulk Densities

ID	Density Level	Specimen Density	Meter Area Density	Difference	Difference
		(kg/m^3)	(kg/m^3)	(kg/m^3)	(%)
059	Low	37.6	38.6	1.7	2.8
072	Low	37.7	38.4	0.7	1.9
168	Low	36.6	38.6	1.7	4.7
176	High	44.2	45.4	1.2	2.8
239	High	44.4	45.4	0.9	2.1
242	High	45.1	45.1	0.1	0.2
242	Low	36.6	38.5	1.9	5.2
260	High	43.8	45.2	1.4	3.3
			Average	1.12	2.8
			Std. Dev.	0.57	1.6

The grand average of the differences and the standard deviation were 1.12 kg/m^3 and 0.57 kg/m^3, respectively (Table 6). A 95 percent confidence interval for the "true" density difference was determined from the following equation

$$\bar{\rho} \pm t_{\alpha/2,DoF}\frac{s}{\sqrt{n}} \qquad (4)$$

where $\bar{\rho}$ and s are the grand average and standard deviation, respectively, (Student's) t for 95 percent and 7 degrees of freedom (DoF) is 2.36, and n is the number of measurements. The corresponding interval was 1.12 ± 0.48 kg/m^3 which does not contain zero. Therefore, the difference in densities for the meter area and the entire specimen was statistically significant and a value of 1.12 kg/m^3 was added to the specimen bulk densities of Table 5 to account for the differences.

Multiple Variable Regression Analysis

Plots of the specimen thermal conductivity as a function of specimen bulk density and mean temperature are shown in Figures 7a and 7b, respectively. The plots indicate that the thermal conductivity was sensitive to changes in (mean) temperature and fairly insensitive to changes in bulk density. For the (corrected) bulk density range of 37.4 to 45.8 kg/m^3, the change in thermal conductivity with respect to bulk density was quite small and gradually decreased as bulk density

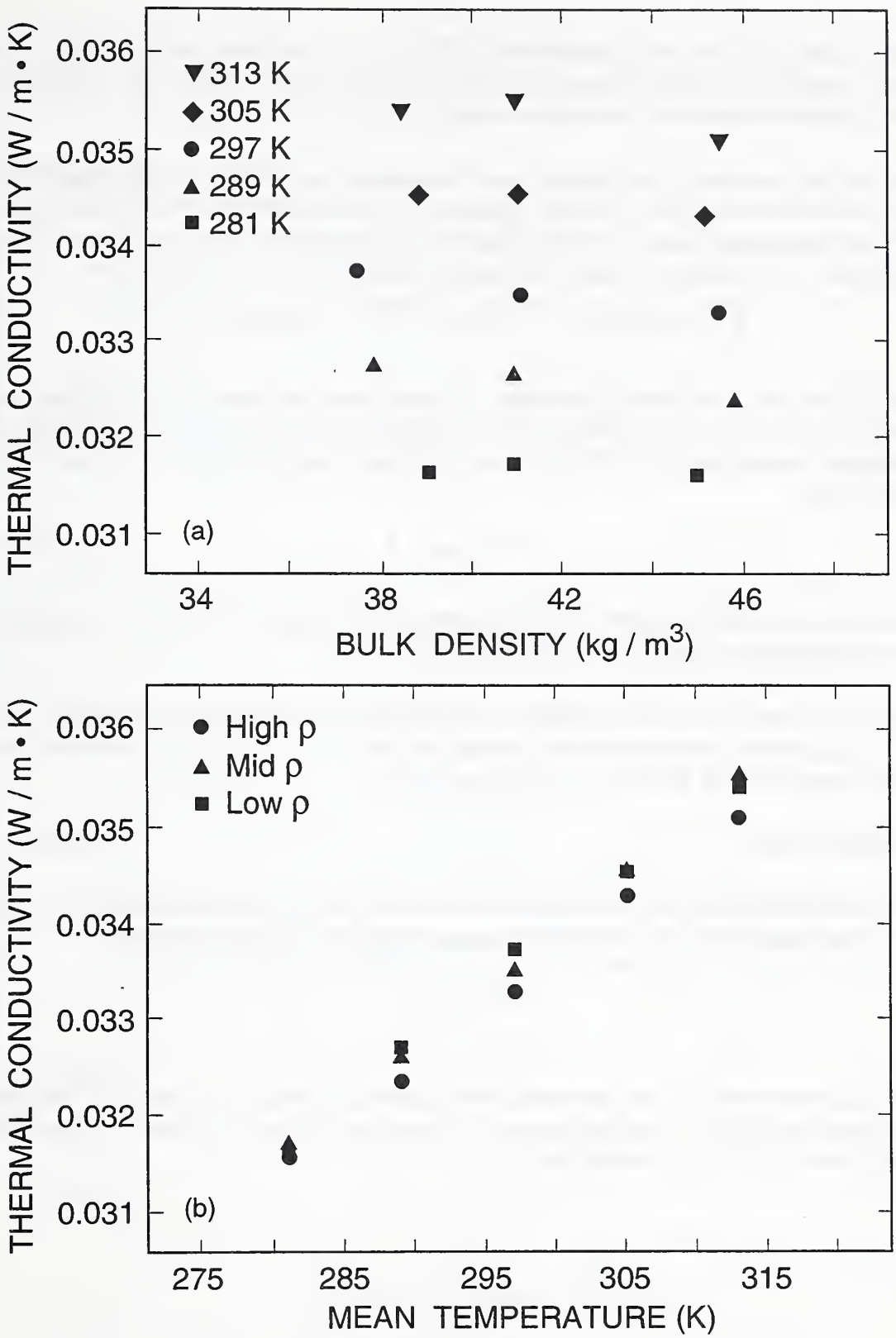

Figure 7 . (a) Thermal conductivity as a function of bulk density.
(b) Thermal conductivity as a function of mean temperature

increased (Figure 7a). Over mean temperatures of 281 to 313 K, the thermal conductivity increased in a linear manner from approximately 0.0316 to 0.0354 W/m·K (Figure 7b). At 297 K, the measured thermal conductivity was approximately 0.0335 W/m·K.

The data for the (corrected) bulk density, mean temperature and corresponding value of thermal conductivity were fit to the $\lambda(\rho,T)$ model, Equation (3), by a multiple variable regression analysis. Higher order temperature terms were determined to be statistically insignificant and a final form, linear in ρ and T, was found adequate. The regression coefficients for the model are

$$\lambda = 6.3028\times10^{-4} - 4.1987\times10^{-5}\rho + 1.1650\times10^{-4}T \quad (5)$$

The last digit of the coefficients is provided to reduce rounding errors. The residual standard deviation for the above fit was 0.000079 W/m·K. The adequacy of the fit was examined by plotting the individual deviations (δ), in W/m·K, from the model versus ρ and T. Values of δ were determined from

$$\delta = \lambda_{meas} - \lambda \quad (6)$$

and plotted versus ρ and T in Figures 8a and 8b, respectively. Figures 8a and 8b do not indicate any trends in the deviations, signifying a satisfactory fit.

The standard uncertainties for the predicted values of λ generally increased at the extreme values of ρ and T (i.e., greater precision near the median values of ρ and T). The maximum standard uncertainty was 0.000048 W/m·K at 37 kg/m^3 and 281 K.

6. Certified Values

Based on the regression analysis of the sample lot, certified values of thermal resistance (R) of SRM 1453 were calculated for a 13.4-mm-thick specimen using the following equation:

$$R = \frac{L}{\lambda} \quad (7)$$

The thermal conductivity (λ) was computed from Equation (5) and the value of 13.4 mm was the grand average from Table 5. Certified values of R are given in Table 7 for ρ and T ranging from 38 to 46 kg/m^3 and 285 to 310 K, respectively.

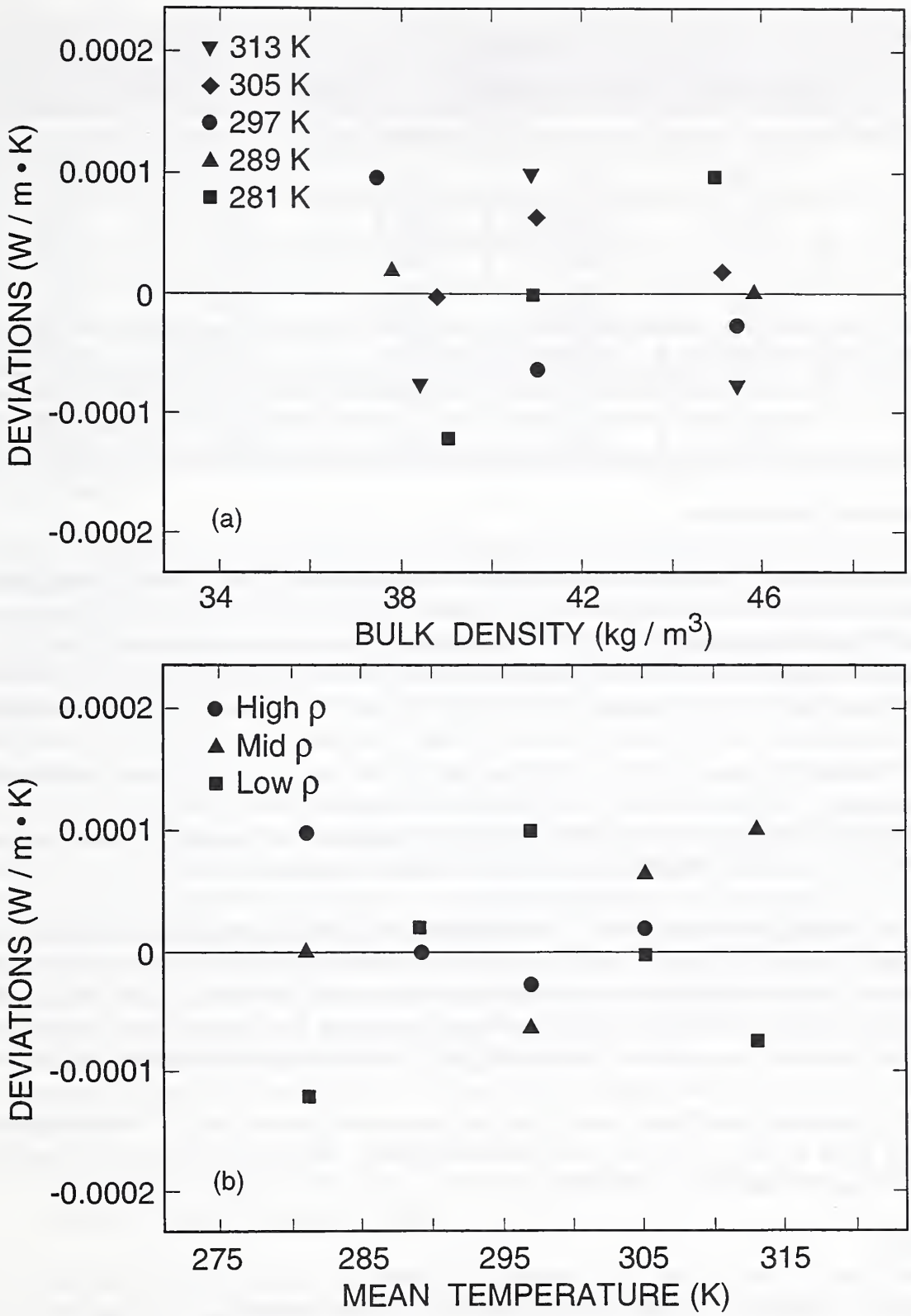

Figure 8 . Scatter plots. (a) Deviations versus bulk density.
(b) Deviations versus mean temperature.

Table 7 Certified Values of Thermal Resistance of a 13.4 mm Thick Specimen					
Temperature (K)	Bulk Density (kg/m^3)				
	38	42	42	44	46
285	0.416	0.418	0.418	0.419	0.420
285	0.408	0.404	0.410	0.411	0.413
285	0.401	0.402	0.403	0.404	0.405
300	0.394	0.395	0.396	0.397	0.398
305	0.388	0.389	0.390	0.390	0.391
310	0.381	0.382	0.383	0.384	0.385

Restrictions and Precautions

The certified values of R in Table 7 are restricted to the measured ranges of bulk density, mean temperature, thickness, and thermal conductivity presented herein. This means that certified values of R are valid only over a density range of 38 to 46 kg/m^3 and a temperature range of 281 to 313 K. Further, the thermal conductivity of polystyrene foam dramatically increases with specimen thickness due to the increased transmission of long-wave thermal radiation in thicker specimens [14,15]. Consequently, certified values of R are *not* valid when specimens of SRM 1453 have been stacked to increase thickness; that is $L \gg 13.4$ mm or, for that matter, $L \ll 13.4$ mm. Values of R from thicknesses of 13.2 to 13.6 (13.4 ± 0.2 mm) can be determined from Equations (5) and (7). As a final note, the boundary conditions of the user application must be comparable to the (normal) emissivity, ϵ, of the surface plates of the guarded hot plate apparatus, $\epsilon = 0.89$.

With reasonable care, specimens of SRM 1453 should have an indefinite shelf life. Guidelines for providing the proper clamping load during testing are provided in Appendix C. For thermal testing, the specimens must be in firm contact with the apparatus plates. However, do not compress the material more than 0.34 mm (2.5 percent) of its original thickness. Polystyrene foam is insensitive to changes in humidity, Appendix D. In the worst case, the moisture content of the foam at 24 °C was found to be less than 1 percent at a relative humidity of 97 percent. The upper temperature of SRM 1453 is limited to the softening point of the polystyrene polymer which is 74 °C [13]. A lower temperature limit for SRM 1453 has not been established. General precautions for handling polystyrene foam are described in Appendix E.

Uncertainty

The expanded uncertainty, U, for certified values of R was determined from the individual contributions of: the curve-fit for the $\lambda(\rho,T)$ model, Equation (5); the standard uncertainty of the thermal conductivity measurement, λ (Appendix A); the correction for the bulk density, ρ, of the meter area (Table 6); and, the uncertainty in the mean temperature measurement (Appendix A). The standard uncertainty for the curve-fit was 0.000048 W/m·K (Section 5). The standard uncertainty

for the measurement of λ was 0.00012 W/m·K (Appendix A). The standard uncertainties for the correction of bulk density and the mean temperature were 0.20 kg/m^3 (Equation A-5) and 0.024 K (Appendix A), respectively. The last two contributions were propagated through Equation (5) to yield a standard uncertainty of 0.000010 W/m·K. The standard uncertainties were combined with the following equation:

$$U = k\sqrt{\sum u(x_i)_A^2 + \sum u(x_i)_B^2} \qquad (8)$$

Taking $k = 2$, provides an interval having a coverage factor that is consistent with international practice. The expanded uncertainty, U, for certified values of λ was 0.00026 W/m·K ($k = 2$). The expanded uncertainty does not include any estimates for uncertainties introduced by the user or long-term drifts in the material.

7. Summary

Thermal conductivity measurements at room temperature are presented as the basis for certified values of SRM 1453, expanded polystyrene board. The thermal conductivity measurements were conducted over range of bulk density of 37.4 to 45.8 kg/m^3 and mean temperature of 281 to 313 K. A model dependent on these two parameters has been developed that describes the thermal conductivity over the range of the parameters. An expanded uncertainty, consistent with current ISO guidelines, has been prepared.

8. Acknowledgments

Several people have contributed to this project over a period of two years. Nancy Trahey and Robert Gettings provided support through the Standard Reference Materials Program. NIST Statistician, Dr. Eric Lagergren provided guidance in the experimental design and data analysis. The surfaces of the foam boards was prepared by Ron Baumgardner of Rollin, Inc. Micrographs of the foam were filmed by Paul Stutzman and compressive resistance measurements provided by James Seiler and Dr. Walter Rossiter. The surface roughness measurements were provided by C.K. Rymes and J.F. Song. Sorption isotherm measurements were supervised by Doug Burch. Chris Saunders assisted with the density measurements of the 300 foam boards.

9. References

1. Taylor, J.K. "Standard Reference Materials, Handbook for SRM Users", *NIST Special Publication 260-100*, February 1993.

2. ASTM. "C 1199 Standard Test Method for Measuring the Steady-State Thermal Transmittance of Fenestration Systems Using Hot Box Methods", *Annual Book of ASTM Standards, Vol. 04.06.*

3. United States Public Law 102-486, 102nd Congress, October 24, 1992.

4. Bowen, R.P. and K.R. Solvason. "A Calorimeter for Determining Heat Transmission Characteristics of Windows", *Thermal Insulation: Materials and Systems, ASTM STP 922*, F.J. Powell and S.L. Matthews, Eds., American Society for Testing and Materials, Philadelphia, 1987, pp. 567-581.

5. Goss, W.P., Elmahdy, H.A. and R.P. Bowen. "Calibration Transfer Standards for Fenestration Systems", *In-Situ Heat Flux Measurements in Buildings: Applications and Interpretations of Results, CRREL Special Report 91-3*, S.N. Flanders, Ed., 1991, pp. 251-260.

6. ASME. "Surface Texture: Surface Roughness, Waviness, and Lay", *ASME B46.1*, draft in preparation.

7. Powell, F.J. and B.G. Rennex. "The NBS Line-Heat-Source Guarded Hot Plate for Thick Materials", *Thermal Performance of the Exterior Envelopes of Buildings - II, ASHRAE SP 38*, 1983, pp. 657-672.

8. Zarr, R.R. and M.H. Hahn. "Line Heat Source Guarded Hot Plate Apparatus", *Adjunct ASTM Practice C 1043*, draft in preparation.

9. ASTM. "C 177 Standard Test Method for Steady-State Heat Flux Measurements and Thermal Transmission Properties by Means of the Guarded Hot Plate Apparatus", *Annual Book of ASTM Standards, Vol. 04.06.*

10. ASTM. "D 1622 Standard Test Method for Apparent Density of Rigid Cellular Plastics", *Annual Book of ASTM Standards, Vol. 08.01.*

11. ISO. *Guide to the Expression of Uncertainty in Measurement*, International Organization for Standardization, Geneva, Switzerland, 1993.

12. Taylor, B.N. and C.E. Kuyatt. "Guidelines for Evaluating and Expressing the Uncertainty of NIST Measurement Results", *NIST Technical Note 1297*, 1994.

13. ASTM. "C 578 Standard Specification for Rigid, Cellular Polystyrene Thermal Insulation", *Annual Book of ASTM Standards, Vol. 04.06.*

14. Booth, J.R. and J.T. Grimes. "The Determination of Radiation k-Factor for Foam Structures Using HFM Apparatus", *Thermal Conductivity 22*, Technomic: Lancaster, Pennsylvania, 1994, pp. 783-793.

15. Jones, T.T. "The Effect of Thickness and Temperature on Heat Transfer Through Foamed Plastics", *Plastics and Polymers*, February 1972, pp. 33-39.

16. Roark, R.J. *Formulas for Stress and Strain*, 4th Ed., 1965, p. 219.

17. ASTM. "C 165 Standard Test Method for Measuring Compressive Properties of Thermal Insulation", *Annual Book of ASTM Standards, Vol. 04.06.*

18. Mehta, S., S. Biederman, S. and S. Shivkumar, "Thermal Degradation of Foamed Polystyrene", *Journal of Materials Science,* Vol. 30, 1995, pp. 2944-2949.

Appendix A

Uncertainty Analysis for Thermal Conductivity (λ)

Background

In 1992, NIST officially adopted a new policy [12] for the expression of measurement uncertainty consistent with international practices set forth in the ISO *Guide to the Expression of Uncertainty in Measurement* [11]. This policy provides a uniform approach at NIST for combining uncertainties and is summarized briefly below. Further details are available in references [11 and 12].

In many cases, a measurand Y is not determined directly from a measurement, but rather mathematically from a function of N other *independent* quantities X_i:

$$Y = f(X_1, X_2, ..., X_N) \qquad \textbf{(A-1)}$$

The output estimate of Y, denoted as y, is obtained using input estimates x_i for the values of the N independent quantities X_i:

$$y = f(x_1, x_2, ...x_N) \qquad \textbf{(A-2)}$$

The combined standard uncertainty of y, $u_c(y)$, is the positive square root of the combined variance, $u_c^2(y)$; where

$$u_c^2(y) = \sum_{i=1}^{N} \left(\frac{\partial f}{\partial x_i} \right)^2 u^2(x_i). \qquad \textbf{(A-3)}$$

Equation (A-3) is commonly referred to as the "law of propagation of uncertainty". The partial derivatives are known as sensitivity coefficients and are equal to $\partial f / \partial X_i$ evaluated at $X_i = x_i$. The corresponding term, $u(x_i)$, is the standard uncertainty associated with the input estimate x_i.

Each $u(x_i)$ is evaluated as either a Type A or Type B standard uncertainty. Type A standard uncertainties are evaluated by statistical means. Type B standard uncertainties cannot be determined directly from the experiment at hand and must be evaluated by other means such as, (previous) measurement data from another experiment, experience, manufacture's specification, etc. [11,12]. Categorizing the evaluation of uncertainties as Type A or Type B is simply a matter of convenience, since both are based on probability distributions[3] and combined equivalently in Equation (A-3). An example of a Type A evaluation is provided below. Examples of Type B evaluations are provided in references [11 and 12]. It should be noted that the designations "A" and "B" apply to the two methods of evaluation, not the type of error. In other words, the designations "A" and "B" have nothing to do with the traditional terms "random" or "systematic".

---

[3] This is not entirely true. The probability distribution for a Type B evaluation, as opposed to a Type A evaluation, is assumed based on the experimenter's judgement.

As an example of a Type A evaluation, consider an input quantity X_i determined from n independent observations obtained under the same conditions. In this case, the input estimate x_i is the sample mean determined from:

$$x_i = \overline{X_i} = \frac{1}{n}\sum_{k=1}^{n} X_{i,k} \qquad \textbf{(A-4)}$$

The standard uncertainty, $u(x_i)$ associated with x_i is the estimated standard deviation of the sample mean:

$$u(x_i) = s(\overline{X_i}) = \frac{s}{\sqrt{n}} \qquad \textbf{(A-5)}$$

When an additional level of uncertainty is required that provides an interval (similar to a confidence interval, for example), an expanded uncertainty, U, is obtained by multiplying the combined standard uncertainty, $u_c(y)$, by a coverage factor, k:

$$U = k u_c(y) = k\sqrt{\sum u^2(x_i)_A + \sum u^2(x_i)_B} \qquad \textbf{(A-6)}$$

The value of k is chosen based on the desired level of confidence to be associated with the interval defined by U and typically ranges from 2 to 3. Interpretation of the coverage factor requires a word of caution. The term "confidence interval" has a specific definition in statistics and is only applicable to intervals based on u_c when certain conditions are satisfied, including that *all* components of u_c be obtained from Type A evaluations. Under these circumstances, a coverage factor of $k = 2$ defines an interval having a level of confidence of about 95 percent and $k = 3$ defines an interval having a level of confidence greater than 99 percent. At NIST, the value of the coverage factor is $k = 2$, by convention [12].

Components of Uncertainty

Referring to Equation (1) in the text, the standard uncertainty for λ was evaluated based on the individual standard uncertainties for the specimen heat flow (Q), meter area (A), specimen temperature difference, (ΔT), and in-situ thickness (L). These individual standard uncertainties were evaluated by either statistical methods (Type A), other means (Type B), or both. Table A-1 identifies the components of the standard uncertainty for λ in **boldface** and the method (Type A or Type B) used to evaluate numerical values. The Type A individual standard uncertainties were evaluated using Equation (A-5) and the Type B individual standard uncertainties were determined by propagation of errors using Equation (A-3). The individual standard uncertainties $u(x_i)$ for Q, A, ΔT, and L were obtained by either error propagation, manufacturer's specification, NIST calibration, calculation, or other measurements (Table A-1). The uncertainty evaluations for Q, A, ΔT, and L are discussed briefly below.

Table A-1 Individual Standard Uncertainties, $u(x_i)$, for Thermal Conductivity				
Variable	Type A		Type B	
	$u(x_i) = s(\overline{X}_i)$	DoF* (n-1)	$u(x_i)$	Source
1. Specimen heat flow, Q	**0.0007 W**	**119**	**0.0103 W**	**Error Prop.**
a) Meter Area Power, Q_m	---	---	0.0065 W	Error Prop.
1) Voltage Measurement	---	---	12.7 mV	Specification
2) Voltage Std. Resistor	---	---	7.7 μV	Calibration
3) Std. Resistor Calibration	---	---	1 ppm, Ω	Calibration
b) Guard Imbalance, Q_g	---	---	.0080 W	Appendix A
2. Meter Area, A	---	---	**3.51×10^{-5} m²**	**Error Prop.**
3. Temperature Diff., ΔT	**0.0002 K**	**119**	**0.047 K**	**Error Prop.**
a) Resistance Measurement	---	---	0.0149 Ω	Specification
b) PRT Calibration	---	---	0.005 K	Calibration
4. Thickness, L	---	---	**2.53×10^{-5} m**	**Error Prop.**
a) Instrument Measurement	---	---	2.54×10^{-6} m	Specification
b) Spacer Stop Calibration	8.45×10^{-6} m	12	3.67×10^{-7} m	$u = a/\sqrt{12}$
c) Repeatability of Calibration	8.97×10^{-6} m	4.9	---	---
d) Plate Flatness	6.57×10^{-6} m	31	---	---
e) Plate Deflection	---	---	2.1×10^{-5} m	Calculation

* Degrees of Freedom

Specimen Heat Flow (Q)

Under normal operation (see Figure 6 in the text), the guard plate and ambient air temperature were maintained such that lateral heat losses (Q_{gap} and Q_{edge}) were reduced to negligible proportions. Under these circumstances, the specimen heat flow (Q) was determined by measuring the DC electrical power input to the meter area (Q_m) of the guarded hot plate. The electrical circuit for the measurement consisted of a standard resistor, nominally 0.1 Ω, in series with the electrical heater of the meter area as illustrated in Figure A1. The corresponding equation for the power input to the meter area is:

$$Q_m = i V_m = \left(\frac{V_s}{R_s} \right) V_m \qquad \text{(A-7)}$$

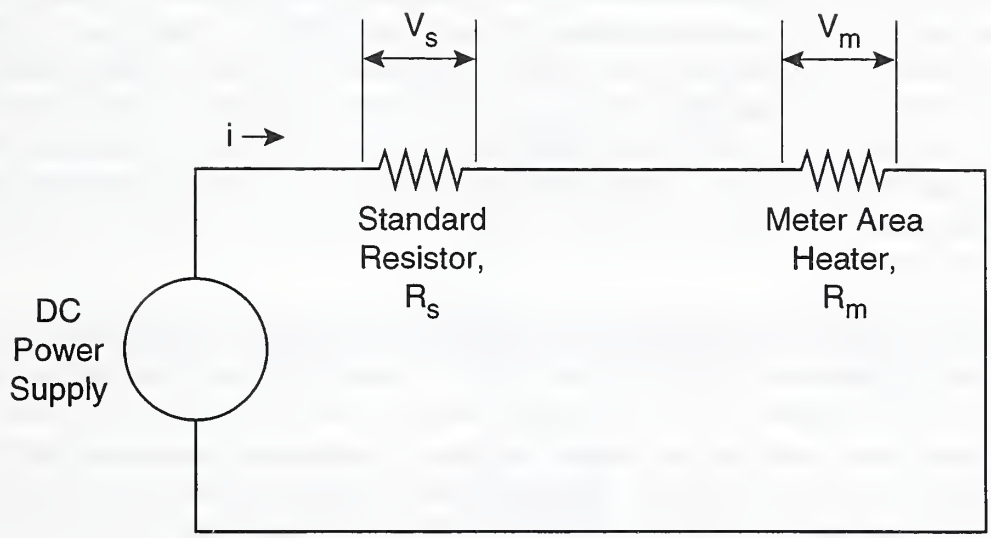

Figure A1. Electrical circuit for meter-area power measurement

where i is the current (V_s/R_s) through the circuit and V_m is the voltage drop measured across the electrical leads to the meter area. The Type B standard uncertainties for V_m, V_r, and R_s are summarized in Table A-1.

The term Q_g in Table A-1 represents both the lateral heat loss at the gap between the meter and guard plates (Q_{gap}) and the heat loss at the edges of the specimens (Q_{edge}). This term was typically quite small (approximately zero) for the fifteen guarded hot plate tests. However, even though the magnitude of Q_g was negligible, an estimate for the standard uncertainty of Q_g was required for the Type B evaluation of the uncertainty of Q. Determining the standard uncertainty for Q_g, required and extensive experimental effort that is described below.

Guard Imbalance (Q_g)

The guard imbalance (Q_g) in a guarded hot plate apparatus refers to heat flow in the lateral direction causing a deviation in the one-dimensional heat flow (Q) through the specimens. Ideally, guarding at the gap and edges of the specimen reduces the lateral heat flows Q_{gap} and Q_{edge} to negligible proportions, Figure 6. An imbalance occurs when a temperature difference develops either across the gap (V_{gap}) or at the edge of the specimens (T_a-T). In our case, V_{gap} and T_a-T refer to the voltage output from a 4-junction Type-E thermopile across the gap and the temperature difference between the ambient air and mean specimen temperatures, respectively. The effect of these two quantities on Q was investigated with a separate series of experiments conducted with the NIST one-meter guarded hot plate apparatus.

Fifteen tests were conducted with a single pair of specimens of expanded polystyrene boards (202 and 207) at mean temperatures (T) of 8, 24, and 40 °C. Following the same installation procedure as the other guarded hot plate tests, the specimens were encircled with fibrous polyester during testing. Five tests were conducted in a random sequence at each mean temperature with V_{gap} and T_a-T each varied at two levels, Figure A2. The experimental design included a center point where V_{gap} and T_a-T were both set to zero; that is, normal operating conditions with negligible heat flows at the gap and specimen edges. This experimental design allowed us to check our previous results and any interaction between the independent quantities. The test sequence for the fifteen tests is summarized in Table A-2.

Table A-2
Test Sequence for Guard Gap and Ambient Temperature Imbalance

T (°C)	T (K)	Number of Tests	Test Sequence (Fig. A2)
8	281	5	4,2,3,1,5
24	297	5	3,5,2,4,1
40	313	5	5,3,4,1,2

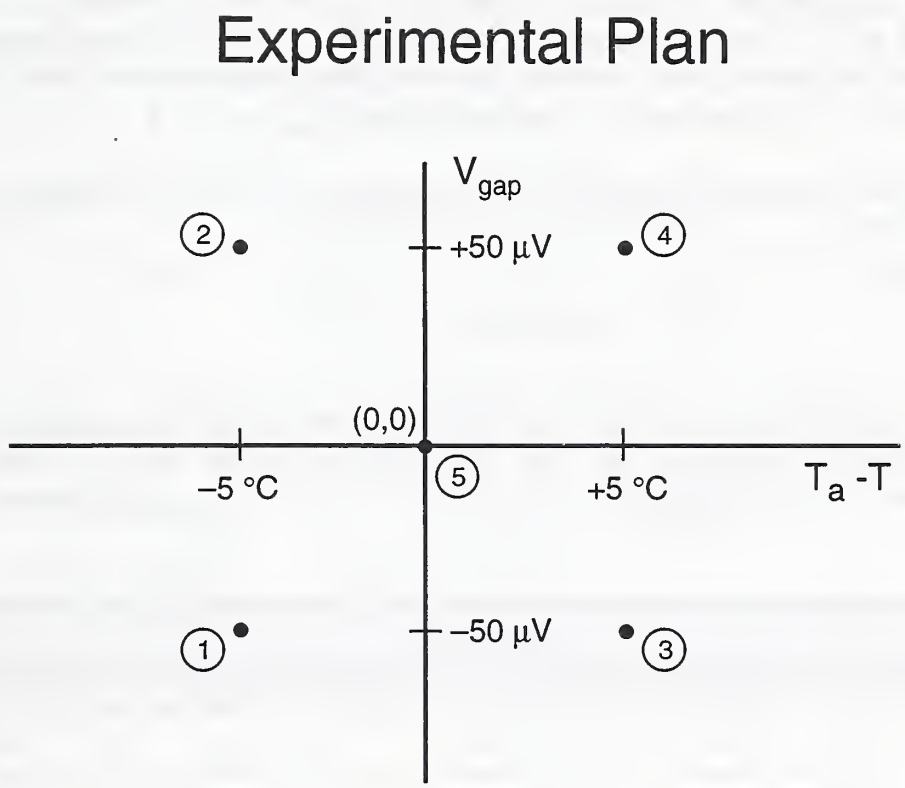

Figure A2. Experimental design for guard gap imbalance and ambient temperatue imbalance.

During each test, the steady-state power input to the meter area (Q_m) of the guarded hot plate was recorded and averaged for the test. The value of the guard imbalance for each test, Q_g, was defined as:

$$Q_g = Q_m - Q_{m_0} \qquad \textbf{(A-8)}$$

where Q_{m_o} was the power input to the meter area when the gap and the edge temperatures were thermally balanced, i.e., at the center point Q_g = zero. The data for Q_m - Q_{m_o} versus V_{gap} and T_a - T are plotted in Figures A3a and A3b, respectively. The change in the power input to the meter area was quite sensitive to change in V_{gap} and fairly insensitive to an imbalance in the ambient air and mean specimen temperatures. A change of ± 50 μV in V_{gap} resulted in an error of ± 0.1 W and a change of ± 5 K in T_a - T caused a change of about 0.02 W. The effect of mean temperature was small as observed in Figures A3a and A3b and the effect of the independent variables on each other was uncorrelated. That is, there was no interaction between V_{gap} and T_a - T.

The data in Figures A3a and A3b were fit to a linear model in V_{gap} and T_a - T at mean temperatures of 8, 24, and 40 °C:

$$Q_m - Q_{m_0} = b_0 + b_1 V_g + b_2 (T_a - T) \qquad \textbf{(A-9)}$$

The coefficients, b_0, b_1, and b_2 were determined by linear regression and summarized in Table A-3. Based on experimental judgement, the Type B standard uncertainty for Q_g in Table A-1 was determined at 24 °C for a gap imbalance of 2.3 μV (0.01 °C) and an ambient temperature imbalance of 0.5 K.

Table A-3
Regression Coefficients for Guard Gap and Ambient Temperature Imbalance

T	b_0	b_1	b_2	RSD*
(°C)	(W)	(W/μV)	(W/K)	(W)
8	-2.505×10^{-3}	2.231×10^{-3}	5.780×10^{-3}	0.0029
24	-1.569×10^{-3}	2.221×10^{-3}	1.882×10^{-3}	0.0017
40	5.07×10^{-4}	2.348×10^{-3}	1.329×10^{-3}	0.0026

*Residual standard deviation

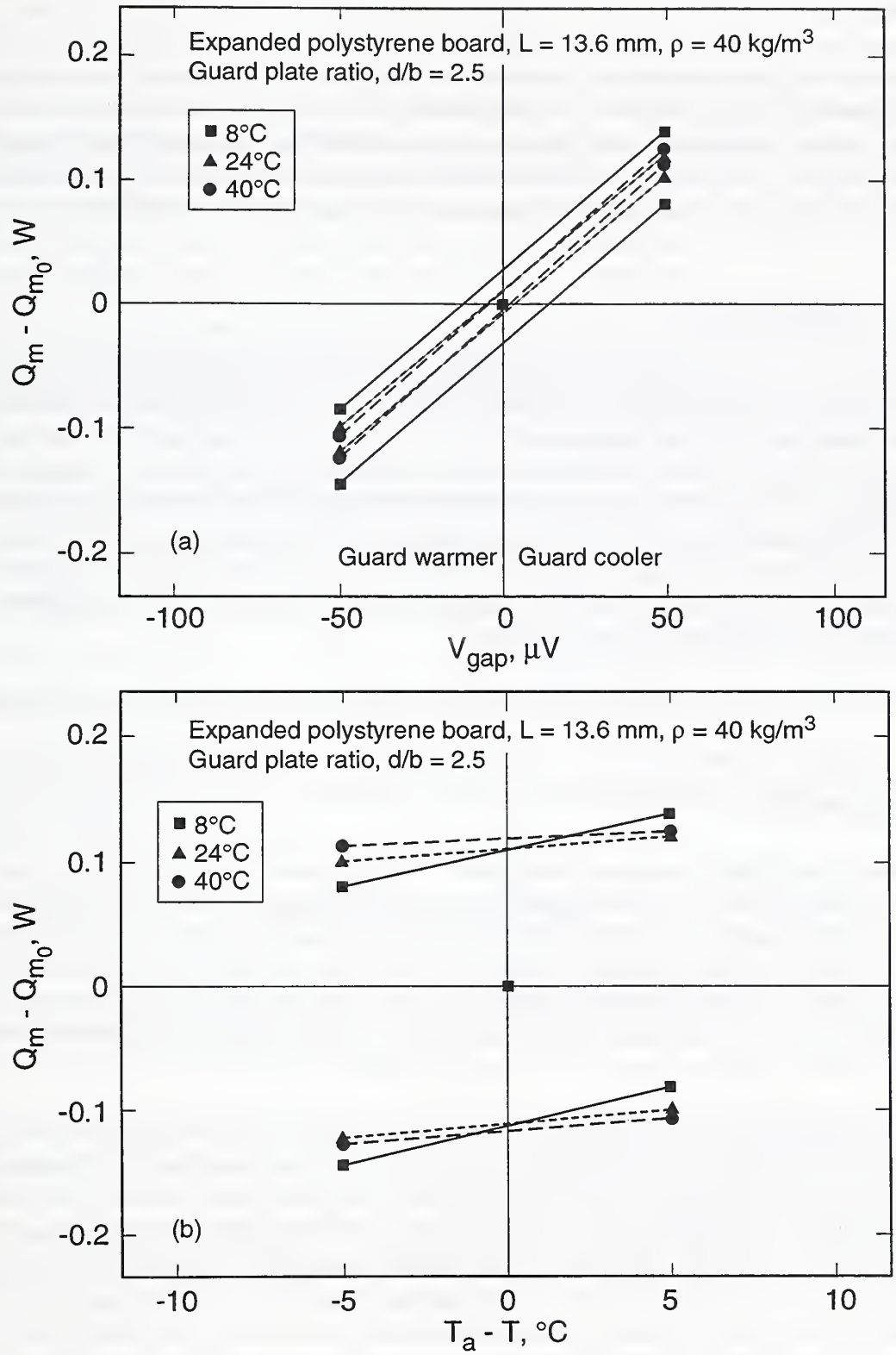

Figure A3. (a) Effect of guard gap imbalance on meter plate power.
(b) Effect of ambient temperature imbalance on meter plate power.

Meter Area (A)

The meter area, at a given temperature, was calculated from the equation: $A = \pi r^2$ where r is one-half the radial distance of the gap between the outer radius (r_o) of the meter plate and the inner radius (r_i) of the guard plate. During testing, the radius (r) was corrected for the effect of thermal expansion, α, of the meter plate. The value of α was taken from handbook data for aluminum, alloy 6061-T6. The uncertainty for A in Table A-1 includes the individual uncertainty contributions for r_o, r_i, and α.

Temperature Difference (ΔT)

The temperatures of the hot plate and cold plates were determined using precision platinum resistance thermometers (PRTs). The electrical resistance of the PRTs was measured with a commercial integrating digital voltmeter (DVM). The standard uncertainty for the resistance measurement of the DVM was obtained from the manufacturer's specifications. This uncertainty was probably overly conservative and contributed heavily to the combined standard uncertainty for λ. The standard uncertainty for the calibration of the PRTs was provided by the NIST Thermometry Group. The temperature difference (ΔT) across the specimens was determined from Equation (A-10) and individual standard uncertainties were propagated using Equation (A-3). The subscripts 1 and 2 in Equation (A-10) refer to the two cold plates.

$$\Delta T = T_h - \tfrac{1}{2} (T_{c_1} + T_{c_2}) \qquad \textbf{(A-10)}$$

In-situ Thickness (L)

The thickness of each pair of specimens was measured during testing using the average of eight (four top and four bottom) linear positioning transducers equally spaced at the periphery of the plates. The linear positioning transducer consisted of a 450-mm Invar scale and slider, and digital indicator. During operation, the slider tracked the distance between the translating cold plate and the fixed guarded hot plate. The corresponding output signal was displayed by the digital indicator having a resolution of 2.5×10^{-6} m. The standard uncertainty in the thickness measurement system, as specified by the manufacturer, was 2.5×10^{-6} m (Table A-1).

The digital indicators were reset by placing four fused-quartz (96 percent) spacers of known thickness between the hot plate and cold plate at the same peripheral locations corresponding to the linear positioning transducers. Fused-quartz was selected for the spacers because of its extremely low coefficient of thermal expansion, 5.5×10^{-7} cm/cm·K. The thickness of each fused-quartz spacer was determined by averaging 4 individual measurements taken with a precision micrometer having a resolution of 2.5×10^{-6} m. The Type A standard uncertainty for the fused-quartz spacers was determined by the square root of the sum of the individual variances (s^2) for these measurements (Table A-1). The Type B standard uncertainty for the fused-quartz spacers was based on the measurement resolution of the micrometer (Table A-1).

The repeatability of the linear positioning transducers was determined from a series of replicate thickness measurements taken over several days using the fused-quartz spacers as reference values. The thickness transducers for the cold plates were initially reset as described above using the four fused-quartz spacers. The cold plate was subsequently opened and closed until the plate was in complete contact again with all of the fused-quartz spacers. The values of the digital indicators were recorded and the procedure was repeated five times. This same procedure was repeated for both plates (top and bottom) and a average thickness was computed for each reading. To check the variation form day-to-day, readings were taken on four different days providing a total of twenty thickness averages. Table A-4 gives summary statistics for each day.

Table A-4
Summary Statistics for Thickness Calibration

Day	Replicates	Day Averages (m)	Within-Day Std. Dev. (m)
1	5	1.266×10^{-2}	5.0×10^{-6}
2	5	1.266×10^{-2}	5.9×10^{-6}
3	5	1.267×10^{-2}	2.0×10^{-6}
4	5	1.267×10^{-2}	5.1×10^{-6}

The standard deviation of the daily averages (s_a) was 7.9×10^{-6} m and the within-day standard deviation (s_d) was 4.7×10^{-6} m. The standard uncertainty was determined to be 8.97×10^{-6} m using Equation (A-11)

$$u(x_i) = \sqrt{(s_a)^2 + \frac{r-1}{r}(s_d)^2} \qquad \textbf{(A-11)}$$

where r = number of replicates per day. The DoF (degrees of freedom) was determined from the Welch-Satterthwaite formula in Reference [12].

The flatness of the meter plate was determined using an xyz coordinate measuring machine (CMM) having an uncertainty of 5.1×10^{-6} m. The thickness of the plate was measured at 32 separate locations over the meter plate and the standard deviation of the 32 measurements was subsequently used to determine the Type A standard uncertainty of the plate flatness. The Type B standard uncertainty for the plate deflection was estimated by a calculation based on a deflection formula provided by Roark [16].

Combined Standard Uncertainty for λ Measurement

The combined standard uncertainty, u_c, for λ was determined using the standard uncertainties in Table A-1 that were fixed during a guarded hot plate test. This included all of the Type B standard uncertainties as well as the Type A standard uncertainties for thickness (L). The Type A standard uncertainties for Q and ΔT were considered redundant because these components were included in the measurement of λ of the fifteen pairs of specimens. Table A-5 summarizes the input quantities, X_i, estimates, x_i, standard uncertainties, u_i, and sensitivity coefficients, c_i, for the specimen heat flow (Q), meter area (A), specimen temperature difference, (ΔT), and in-situ thickness (L). The Type B combined standard uncertainty, u_c, for λ was 0.00012 W/m·K.

Table A-5
Combined Standard Uncertainty for Thermal Conductivity Measurement

Quantity, X_i	Estimate, x_i	$u(x_i)$	Sensitivity Coefficients, c_i	Uncertainty (W/m·K)
Q	6.5225 W	0.0103 W	5.14×10^{-3} $m^{-1}K^{-1}$	0.00005
A	0.1297 m^2	3.51×10^{-5} m^2	-0.258 $Wm^{-3}K^{-1}$	0.00001
L	0.01332 m	2.53×10^{-5} m	2.514 $Wm^{-2}K^{-1}$	0.00006
ΔT	20.00 K	0.047 K	1.67×10^{-3} $Wm^{-1}K^{-2}$	0.00008
λ	0.03349 W/m K		**Total**	0.00012

Mean Temperature (T)

The mean temperature was determined from the Equation (A-12)

$$T = \tfrac{1}{2}\left(T_h + \tfrac{1}{2}\left(T_{c_1} + T_{c_2}\right)\right) \qquad \textbf{(A-12)}$$

The standard uncertainty of T was 0.024 K and was determined by propagation of errors using Equation (A-3).

Appendix B

Uncertainty Analysis for Bulk Density (ρ)

The Type A and Type B standard uncertainties for the determination of specimen bulk density are summarized in Table B-1. The Type A standard uncertainties for the length measurements were computed from a relatively small number of measurements. The Type B standard uncertainties for the length measurements were assumed to have a uniform distribution in the interval *a*; where *a* was the smallest length interval of the scale. In the propagation analysis, the Type A standard uncertainties were neglected. The combined standard uncertainty, u_c, for the bulk density was 0.10 kg/m^3 as summarized in Table B-2.

Table B-1
Standard Uncertainties, $u(x_i)$, for Bulk Density Measurements

	Type A		Type B	
Variable	$u(x_i) = s(\overline{X}_i)$	Degrees of Freedom (n-1)	$u(x_i)$	Source
Mass, x_1	---	0	0.1 g	Manufacturer
Length, x_2	0.03 mm	2	0.14 mm	$u(x_2) = a/\sqrt{12}$
Length, x_3	0.03 mm	2	0.14 mm	$u(x_3) = a/\sqrt{12}$
Thickness, x_4	0.007 mm	4	0.029 mm	$u(x_4) = a/\sqrt{12}$

Table B-2
Combined Standard Uncertainty for Bulk Density

Variable	Value	$u(x_i)$	Sensitivity Coefficients, c_i	Uncertainty (kg/m^3)
Mass, x_1	230.0 g	0.1 g	172.8 m^{-3}	0.02
Length, x_2	657.5 mm	0.14 mm	-60.4 kg m^{-4}	0.01
Length, x_3	657.0 mm	0.14 mm	-60.5 kg m^{-4}	0.01
Thickness, x_4	13.4 mm	0.029 mm	2965 kg m^{-4}	0.10
Bulk Density, ρ	39.7 kg/m^3		**Total**	0.10

Appendix C

Compressive Resistance of Expanded Polystyrene Foam

The compressive resistance of SRM 1453 was determined in accordance with ASTM Test Method C 165 [17], Procedure A, using a universal testing machine. The purpose was to provide users of SRM 1453 a maximum pressure limit before the material would mechanically yield, i.e., deform permanently. Seven cylindrical specimens, 100 mm in diameter by 13 mm thick, were cut from board 049 and conditioned in an environment of 23 ± 0.8 °C and 53 ± 0.2 percent relative humidity (aqueous salt solution) for about four months to a steady mass[4]. Since the compressive resistance is a function of bulk density, the specimens were specifically selected from the lowest densities available. That is, the measured compressive resistance would be expected to represent the low end of the range of the SRM.

During testing, the machine was operated at a crosshead speed of 1 millimeter per minute. The compressive load and corresponding deformation were sampled in real-time at a rate of 9.1 points per second in order to construct a load-deformation curve for each specimen. Using a straightedge, the straight portion of the curve was extended to the x-axis, establishing a "zero deformation point". All deformations were determined with respect to this (zero) point. The compressive resistance was determined from:

$$S = \frac{W}{A} \qquad \text{(C-1)}$$

where;

W = compressive load at a given deformation and,
A = original (undeformed) area, m^2.

The compressive resistance for the 7 specimens at an average deformation of 0.34 mm (2.5 percent) is summarized in Table C-1. Above this value, the specimens yielded.

[4] For the conditions specified, steady mass was actually obtained in about 11 days.

Table C-1 Compressive Resistance of Specimens of SRM 1453, Expanded Polystyrene Board						
ID	**Bulk Density**	**Undeformed Area**	**Deformation**	**Strain**	**Load**	**Compressive Resistance**
	(kg/m^3)	**(m^2)**	**(mm)**	**(%)**	**(N)**	**(kPa)**
1	31.8	0.00785	0.33	2.5	2474	315.0
2	32.6	0.00778	0.27	2.0	2275	292.6
3	30.8	0.00781	0.33	2.5	2121	271.4
4	31.8	0.00781	0.38	2.8	2469	316.0
5	32.2	0.00785	0.38	2.6	2667	339.6
6	31.2	0.00785	0.35	2.6	2375	302.4
7	29.5	0.00785	0.36	2.7	2307	293.7
Average	31.3	0.00783	0.34	2.5	2384	304.4
Std. Dev.	1.0	0.00003	0.03	0.3	175	21.7

Appendix D

Sorption Isotherms for Expanded Polystyrene Foam

Sorption isotherms for expanded polystyrene foam were determined using fixed-point humidities provided by aqueous salt solutions. To increase the surface area and thus enhance the sorption process, small rectangular billets, 0.5 by 2 by 13 mm, of foam were cut. One set of billets was prepared for adsorption measurements; the other for desorption measurements. Both sets of foam billets were conditioned in an environment over calcium-chloride desiccant to obtain a "dry" or tare mass. The billets for desorption were subsequently removed from the desiccant containers and placed over distilled water. A fixed number of billets from each set were subsequently placed in containers at 11, 33, 43, 58, 79, 84, 94 and 97 percent relative humidity at laboratory temperature of 24 °C.

The billets from each container were collectively removed and weighed to monitor changes in mass due to sorption of water vapor. The weighing process was repeated until the conditioned mass of the billets achieved a steady value (i.e., less than 1 percent change over a 2-day interval). The equilibrium moisture content ($\gamma\{\phi\}$) was determined by taking the differences between the conditioned mass ($m\{\phi\}$) and initial mass (m_i) and dividing by (m_i), Equation (D-1).

$$\gamma(\phi) = \frac{m(\phi) - m_i}{m_1} \qquad \textbf{(D-1)}$$

For the relative humidity range of 11 to 94 percent, $\gamma(\phi)$ was found to be less than 0.4 percent and less than one percent at 97 percent relative humidity.

Appendix E

General Precautions for Expanded Polystyrene Foam

Upper Temperature Limit

Polystyrene is a thermoplastic and, by definition, has a well-defined temperature at which the polymer softens. The upper temperature limit before cellular polystyrene foam softens, as specified in the ASTM Specification C 578 [13], is 74 °C. Mehta et al. [18] reported that similar polymer polystyrene beads when exposed to elevated temperatures collapsed about 110 to 120 °C. The collapsed beads melted at 160 °C and began to vaporize above 275 °C [18].

Flammability

Standard Reference Material 1453 is a commercial grade of expanded polystyrene foam that does not contain fire-retarding additives. It is an organic thermoplastic material that is combustible and, at elevated temperatures melts (> 160 °C, [18]). For safety, do not expose the material to sources of ignition.

Solvents

Polystyrene is soluble in many organic solvents such as chlorinated and aromatic hydrocarbons, esters, and ketones. The aromatic chemical structure of polystyrene is inherently water repellant. As noted in Appendix D, the material is very insensitive to low levels of humidity.

Ultraviolet Degradation

When exposed to sunlight (ultraviolet radiation), polystyrene degrades as evidenced by discoloration of the surface. To minimize degradation, protect SRM 1453 by covering when exposed to direct sunlight.